How do we efficiently generate high-resolution hydraulic models at large numbers of riverine reaches?

Authors[1]: Matthew Nahorniak[1], Joe Wheaton[2], Carol Volk[1], Phillip Bailey[3], Matt Reimer[3], Eric Wall[4], Kelly Whitehead[1], Chris Jordan[5]

[1] Corresponding Author
matt@southforkresearch.org
South Fork Research, Inc.
44842 SE 145th St.
North Bend, WA 98045 USA

[2]Utah State University

[3]North Arrow Research

[4]EcoLogical Research, Inc.

[5]Northwest Fisheries Science Center

[1] Matthew Nahorniak contributed to model conception and design, data interpretation and drafting the manuscript. Joe Wheaton and Eric Wall contributed to the conceptual modeling approach and data interpretation. Carol Volk and Chris Jordan contributed to the conceptual modeling approach and writing. Kelly Whitehead, Matt Reimer, and Philip Bailey contributed to data acquisition, cloud services architecture and data interpretation.

21

Abstract

In support of efforts to quantify relationships between juvenile salmonid habitat and population dynamics in the Pacific Northwest, over 2200 hydraulic models were generated at more than 900 individual reaches with unique bathymetry. Hydraulic models generated two dimensional field estimates of depth and velocity for each survey, providing a key linkage used to relate bathymetry and habitat data to juvenile salmonid population dynamics. Generating more than 2200 hydraulic models required development of an automated process to generate input files specifying bathymetry, computational grids, and boundary conditions for the Delft3D Flow software (which we run in 2D, and hereafter refer to as “Delft Flow” for clarity), enabling batch-processing of large numbers of hydraulic models, which is the novel advancement we present here. Hydraulic model inputs included digital elevation models (DEM) from topographic surveys, estimates of surface roughness based on pebble size distributions, and discharge. Outputs included velocity vector and depth fields estimated on a rectilinear grid of 10 cm spacing between grid points. Modeled velocities and depths were in reasonable agreement with field-collected velocities and depths. Certain topographic features, such as undercut banks and porous structures not represented in the DEM, resulted in modeled values that failed to reflect accurate velocities but were explained by the presence of these features. By utilizing a rectilinear grid, scaling grid spacing to computational resource limitations, leveraging a cloud computing system, and selecting simplified rules for discharge distribution for boundary conditions and model run times, we were able to successfully automate the hydraulic modeling process. Overall, automation of hydraulic model generation met precision and accuracy needs of habitat condition models, lowered labor costs, and standardized the modeling workflow, and enabled high survey volume processing needs.

Keywords

Hydraulic model, salmon, steelhead, automation

1.1 Introduction

Hydraulic models have been used to effectively estimate velocity and depth fields in stream reaches suitable for juvenile salmonid production (Leclerc et al., 1995; Schwartz et al., 2015; Hayes et al., 2007; Pasternack et al., 2006). A hydraulic model, for our purposes, is defined as field estimates of depth and velocity for the entire stream reach, which is a length of stream of approximately 20 times the bankfull width of the stream that includes the wetted area and adjacent floodplains. Hydraulic models have been developed and studied in terms of their relationship with aquatic organisms (Shen and Diplas, 2008) and are traditionally run on individual reaches, with detailed input, and are manually, highly customized to optimize reach-specific topography, roughness, and hydraulic conditions. Our challenge was to develop an automated process to run multiple hydraulic models for thousands of surveyed riverine reaches in support of the Columbia Habitat Monitoring Program (CHaMP[2]) (CHaMP, 2015), in the Pacific Northwest of the United States. While significant advancements enabling automated hydraulic modeling strategies have been made in recent years (Olivera and Maidment, 2000; Gupta et al., 1999; Yagecic and Suk, 2014), to our knowledge high precision hydraulic modeling

[2] Abbreviations:
CHaMP: Columbia habitat monitoring program
NREI: Net rate of energy intake
HSI: Habitat suitability index
DEM: Digital elevation model
WSEDEM: Water surface elevation digital elevation model

at thousands of unique stream reach surveys as part of an integrated sampling plan has not been previously accomplished.

Two dimensional models of water velocity and depth from hydraulic models have been used to inform models of instream conditions describing fish habitat characteristics (Booker et al., 2004; Kelly et al., 2012) as well as one dimensional models (Tranmer et al., 2018, Benjankar et al., 2018). For example, fish carrying capacity can be estimated from the net rate of energy intake (NREI) (Hayes et al., 2007); and habitat suitability index (HSI) models that consider depth, depth-averaged velocity, and other reach level information to estimate carrying capacity (e.g. Maret et al., 2006; Rubin et al., 1991; Lacey and Millar, 2004) (Figure 1). Such depth and velocity estimates must be at sufficiently fine spatial resolution to adequately link velocity and depth fields to fish biology (Tullos et al., 2016). Hydraulic modeling results are able to provide this level of precision and can be scaled up to stream network level estimates of habitat capacity (Wheaton et al., 2017). Automation of the hydraulic modeling process enables these network level scale ups to be done in a statistically valid manner consistent with a complex, large scale sampling design.

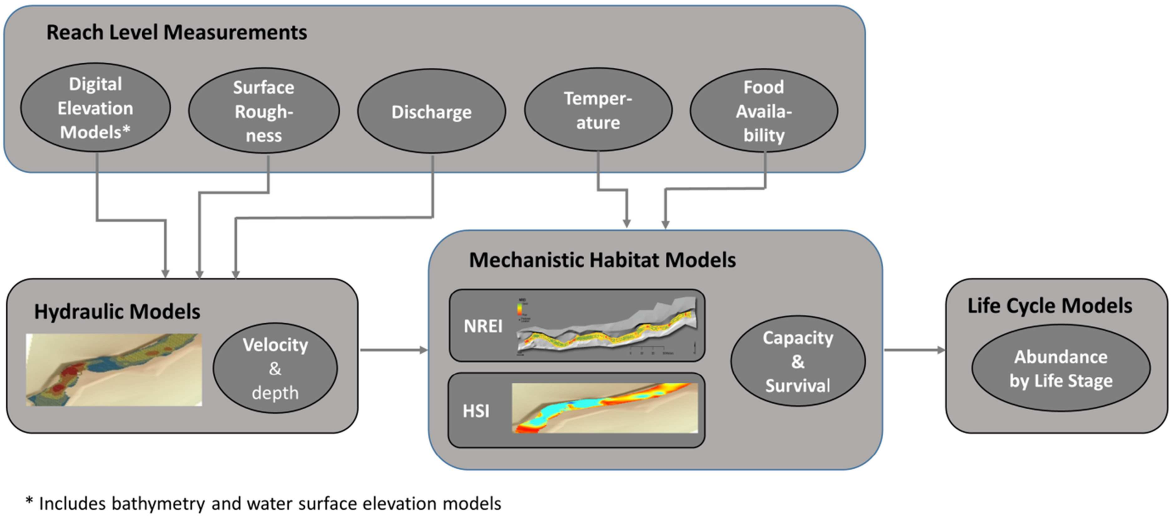

Figure 1. Data flow from reach level measurements to life cycle modeling, indicating how field survey data inform hydraulic models, which in turn inform habitat models such as net rate of energy investment (NREI) and habitat suitability index (HSI) models.

Since 2011, over 2200 sampling events at more than 900 unique stream reaches have generated both topographic and instream habitat data as part of the Columbia Habitat Monitoring Program (CHaMP), a program designed to evaluate status and trends of instream habitat for Endangered Species Act - listed salmon and steelhead populations in the interior Columbia River basin (Bouwes et al., 2011). Note that many unique reaches have been sampled more than once, but in different years, yielding different bathymetry and discharge and necessitating a unique hydraulic model. An automated hydraulic modeling process capable of efficiently producing hydraulic models would allow estimation of habitat capacity throughout the interior Columbia River basin. Our primary objectives were to 1) estimate depth and velocity fields for each unique topographic survey, 2) provide quality assurance feedback informing the accuracy of each model; and 3) retain accurate and spatially fine results of each model.

2.1 Methods

2.1.1 Delft Flow software

We used Delft Flow (http://oss.deltares.nl/web/delft3dto) to model fluid dynamics at each surveyed reach. It is an open source, freely available software with flexible modeling capabilities for free surface flows across a wide range of spatial scales (Deltares, 2013a). It is capable of batch process modeling hydraulic models. Delft Flow requires descriptions of modeled geometry, boundary conditions, initial conditions, fluidic properties, and numerical parameters, input as a series of text files (Deltares, 2013a). We used a rectangular grid with uniform grid spacing in X and Y directions with a fine mesh spacing. After early experimentation with curvilinear grids, we determined the optimal balance of effort – whereby we balance computational time against manual manipulation and optimization of curvilinear grids – was achieved by using a simple rectangular grid with fine mesh spacing throughout a reach.

While the bathymetry data from which we develop our hydraulic models on is 10 cm resolution, the actual survey point density from which the DEMs are generated is significantly less than 10 cm resolution. Field crews take survey points that rely on surveyor judgment to select appropriate point sampling locations and point densities, allowing the surveyor to increase point density in areas with greater topographic complexity or to detail features of interest, and decrease point density in areas with homogeneous topography and of less geomorphic interest (Bangen, 2013). This topographically stratified sampling method approach (Brasington et al., 2000;

Fuller et al., 2003) was used in all surveys with breaks in slope and topography complexity guiding point density stratification. The resulting DEM therefore accurately locates locations of sharp change in bathymetric surface geometry, but features on the scale of 10 cm such as rocks, wood, or vegetation are not included in the bathymetric survey. The resulting DEM is therefore a smoothed out representation of reality, and features such as rocks are accounted for in the hydraulic model as surface roughness rather than directly modeled features. Given this survey strategy, we generally expect features of approximately 30-50 cm (x, y or z axis) or greater to be included in the survey and represented by the DEM. This minimum feature size scales with the length of the reach surveyed; smaller reaches will have minimum feature sizes at the small end of this range while larger reaches will have minimum feature sizes at the large end of this range. This feature size is also dependent on the frequency and distribution of the feature within a reach; unique features are likely to be captured as elements adding complexity with high point densities while high frequency features are more likely to be captured as homogenous topography.

Modeling a smoothed over bathymetric surface and using a surface roughness model lends itself to accepting a depth averaged two-dimensional hydraulic model rather than modeling in full three dimensional space. In addition, Delft-Flow documentation suggests that "[Non-tidal rivers] are generally well-mixed and you can rely on a 2D (depth averaged) computation, unless the project requires the vertical profile of some quantities." (Deltares, 2013a). While vertical profiles of velocity may be of interest around small features such as rocks, this bathymetric information was not available and would therefore not achieve significant enhancements to our models by attempting to model in three-dimensions. In addition, two-dimensional depth averaged models have been shown previously to successfully support NREI (Hayes et al., 2007) and HSI models (Maret et al., 2006; Rubin et al., 1991; Lacey and Millar, 2004). Our objective here was not to enable refinements or improvements to NREI or HSI modeling methods by providing full three dimensional solutions, but rather to enable high volume NREI and HSI modeling by providing thousands of two-dimensional models of equivalent quality to those previously found to be useful and informative for quantifying fish habitat.

2.2 Hydraulic model input data: Columbia Habitat Monitoring Program

The Columbia Habitat Monitoring Program utilizes a spatially balanced statistical sampling design (Stevens and Olsen, 2004) to monitor wadeable streams and rivers accessible to anadromous steelhead (Oncorhynchus mykiss) and/or Chinook salmon (Oncorhynchus tshawytscha) (CHaMP, 2015) (Figure 2). Most stream reaches have been sampled over multiple years in order to assess temporal changes to topography and features, thereby requiring unique hydraulic model for each survey. Carrying capacity and productivity are used as the basis for models of salmonid population dynamics (Moussalli and Hilborn, 1986) used by the program and a hydraulic model provides continuous depth and velocity fields as inputs to such models.

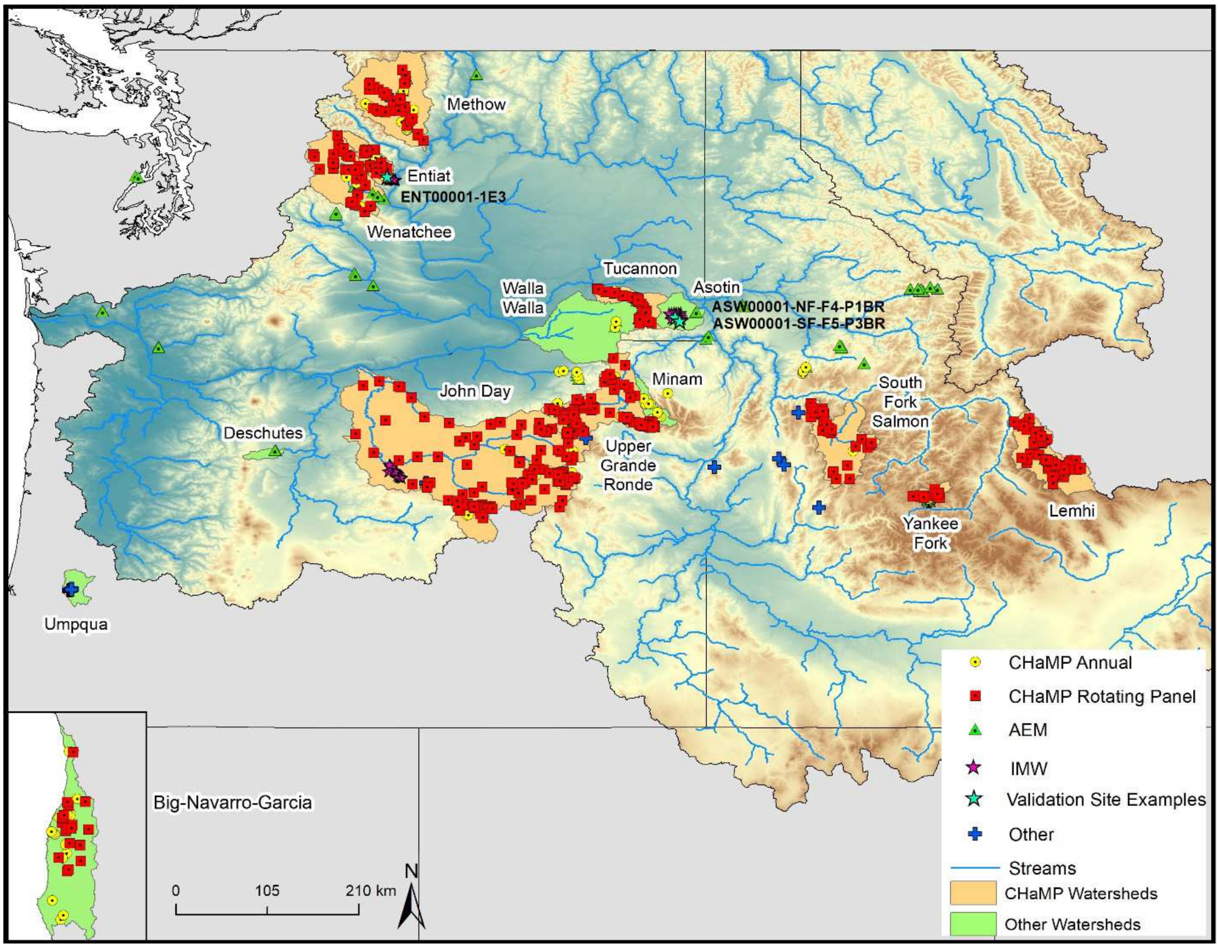

Figure 2. Location of surveyed reaches within the Columbia River basin as part of the CHaMP, AEM (Action Effectiveness Monitoring), and IMW (Intensively Monitored Watersheds) programs.

The hydraulic models utilized digital elevation models (DEMs, 10cm resolution) from high precision ground based topographic surveys (Bouwes et al., 2011). Such ground based surveys have become common sampling tools in fluvial geomorphology (Wheaton et al., 2010) and have demonstrated low measurement variability (Bangen et al., 2014). For each reach, DEMs were produced for both reach-level bathymetry and water surface elevation, along with a thalweg.

Field crews also measured pebble size distributions (D84) and discharge (Bouwes et al., 2011) which we leverage in our hydraulic modeling process. Discharge rates (m^3/s), represent low flow conditions as sampling occurs in the summer months (July-September).

2.3 Hydraulic modeling work flow

DEM and related field data are processed with R scripts (R Core Team, 2014) and Delft Flow to generate a hydraulic model for each stream reach (Figure 3). A pre-processing script is used to generate the numeric grid (step 1), build the required Delft Flow input files, (step 2), and set up the required files and file structures for batch processing (step 3). Delf3d Flow is then run in batch mode (step 4), and outputs are converted into text format (step 5) and then post-processed to generate final depth and velocity outputs (step 6). We review outputs for quality (step 7) and final results are stored in an online data warehouse (step 8). The required Delft Flow inputs consist of a series of input files describing, among other things: bathymetry, surface roughness, boundary conditions, initial conditions, and numeric constants, as well as a master definition file (Table 1). R-code, example input files, and documentation are available at: https://github.com/SouthForkResearch/Hydraulic-Modeling

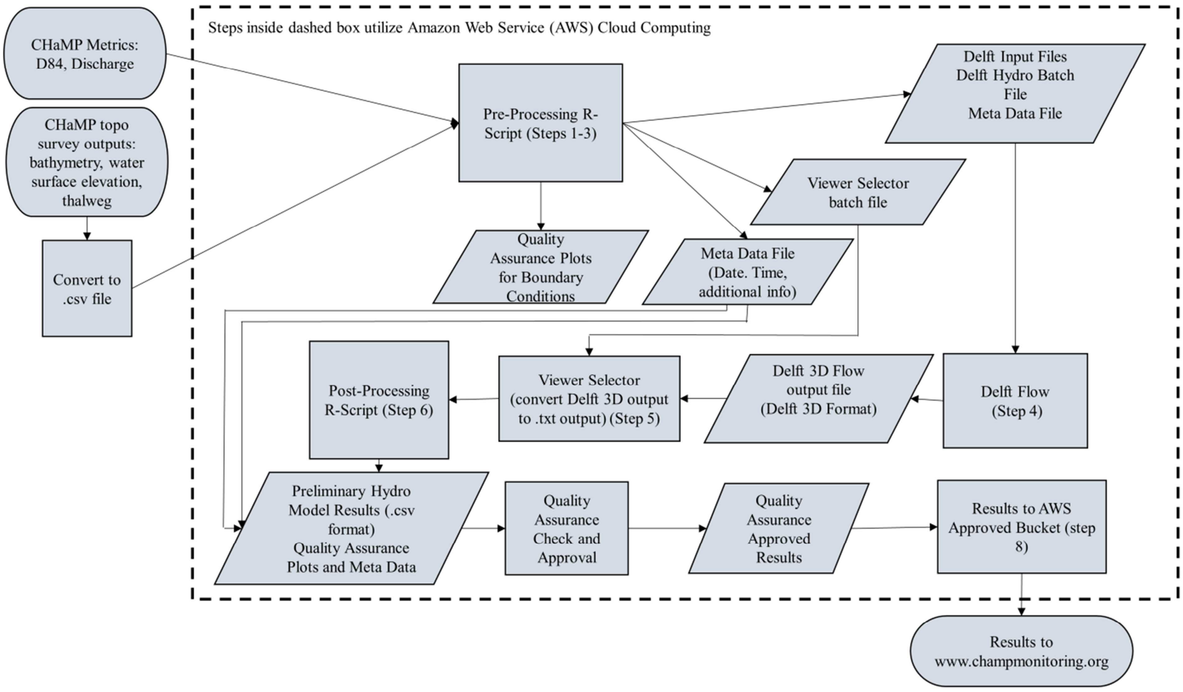

Figure 3. Hydraulic modeling work flow

Delft Flow Input File Created by Pre-Processing R Script	Description
test.grd	File defining the numerical grid
test.enc	Grid enclosure file
test.dry	Dry points file
test.dep	Bathymetry
test.bct	Downstream boundary condition locations
test.bnd	Downstream boundary condition
test.src	Discharge locations
test.dis	Discharge rates
test.mdf	Master definition file; lists filenames for all other input files and contains key physical and numerical constants

Table 1. Delft Flow input files generated using a pre-processing R script

2.3.1 Step 1: define the numeric grid used by Delft Flow

The first pre-processing step is to develop the numerical grid. A rectangular grid with extents in the cardinal directions equal to the maximum and minimum extents of the surveyed DEM is first generated. Over this rectangle we plot the thalweg and determine the closest edge (North, South, East, or West) to the upstream and downstream ends of the thalweg (Figure 4). The trend in water surface elevation along the thalweg can be used to identify which boundary is upstream and which is downstream. Note that the inlet and outlet can occur on the same edge of the computational grid.

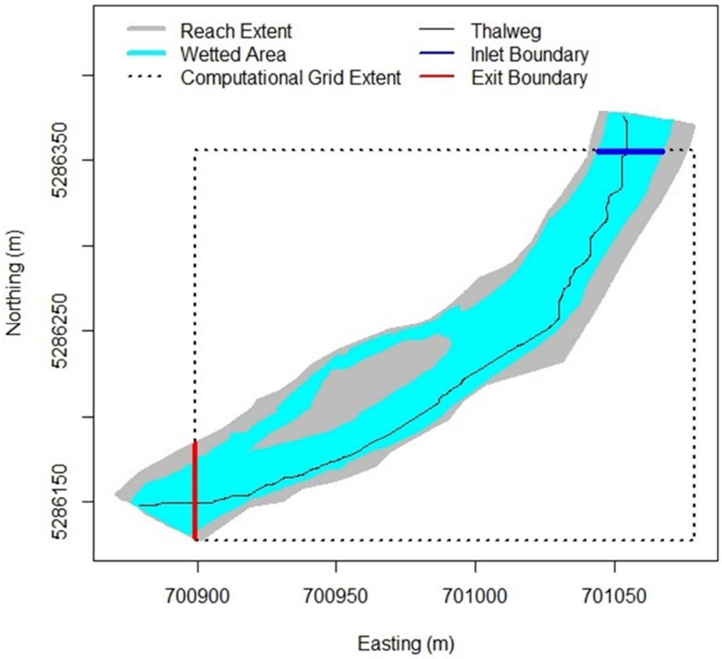

Figure 4. Extent of reach surveyed, computational grid and inlet/exit boundary location for example reach ENT00001-1E3

The inlet and outlet boundaries are then trimmed by user-defined extents (2m default) to ensure that the edges of the computational grid cross wetted edges of the reach at both the inlet and outlet boundaries (Figure 4). While this trimming step results in some loss of total area modeled, it allows efficient and automated definition of computational grid boundaries without a priori knowledge or manual user specification of upstream and downstream edges.

By using a rectangular grid outlining the stream reach, we necessarily include a significant area in our computational grid that is not part of the surveyed stream reach (Figure 4, white area within the computational grid). Grid points outside the reach are defined as dry points, and are not included in Delf3D Flow calculations, reducing required computational power.

Models are limited by computer memory requirements and can be consistently run on computational grids containing approximately 500,000 grid points. Our algorithm therefore varies the grid spacing by the size of stream reach being modeled and uses as fine of a grid as possible without exceeding that limit. Additionally, grid spacing is set at either a multiple or an integer fraction of the 10 cm DEM grid spacing, simplifying and minimizing systematic error in the interpolation between the DEM and computational grid. We ensured the computational grid spacing was sufficiently fine by comparing simulation results at the grid spacing, as determined by our 500,000 cell limit, to those run at two and four times the 500,000 cell limit algorithm-based grid spacing. Our grid spacing algorithm ensured that our computational grid spacing was finer than the effective minimum feature size surveyed, as described above.

2.3.2 Step 2: generation of Delft Flow input files for bathymetry and boundary conditions

The pre-processing script generates Delft Flow input files specifying the bathymetry ("test.dep"), downstream boundary conditions ("test.bnd" and "test.src"), and the distribution of discharge at the upstream boundary ("test.src" and "test.dis"), as well as initial conditions, required simulation times, and a master definition file (test.mdf) describing surface roughness, fluidic properties of water and time step information. We used a horizontal eddy viscosity of 0.01 m^2/s and a diffusivity of 10 m^2/s. Our time step is set at 0.0025 seconds for all models and was selected as a sufficiently fine time step that enabled stable numerical solutions in all cases with the minor expense of numerical efficiency that could be achieved if a time step were optimized for each individual model. The Courant-Friedrichs-Lewy number, at this time step and for typical depths of approximately 1 meter, is about 0.75. The Delft Flow manual (Deltares, 2013a) suggests keeping this value below 10 to ensure accuracy and numerical stability. We chose to stay well below this, although efficiencies may be gained by attempting to optimize this value. The Delft input file for bathymetry ("test.dep") is generated by spatially interpolating bathymetry from the DEM grid onto the computational grid, unless the computational grid point lands exactly on the DEM grid point, in which case the values are transcribed exactly. Since both grids are rectangular and uniformly spaced, the four nearest DEM points form a square, within which the computational grid point is located, making for easy interpolation. The downstream boundary condition (specified in files "test.bnd" and "test.bct") specifies the water surface elevation at the exit boundary and is specified as the thalweg water surface elevation where the thalweg crosses the exit boundary. Discharge is distributed across the wetted length of the computational upstream boundary and is defined in the "test.src" and "test.dis" files. The total discharge is distributed along each cell of the inlet boundary such that the volume flow rate at each cell was proportional to the measured water depth.

Because the inlet and outlet boundary conditions are specified at edges along cardinal directions, there is often boundary condition specification error as the flow direction is rarely orthogonal to the boundary. In some cases, the wetted boundary edge extends across multiple edges (e.g. north and west edges). Experimentation with boundary conditions suggested that boundary condition errors typically propagated no more than one or two wetted widths from the inlet or exit boundary, which is a small fraction of the overall stream length modeled for modeled stream reaches (CHaMP, 2015).

We recognize that boundary condition errors for both upstream and downstream boundaries could potentially be reduced by using a curvilinear computational grid, which would allow the boundaries to be more perpendicular to flow directions. We prioritized simplicity over boundary condition precision to enable high volume modeling. Early work developing curvilinear grids resulted in high rates of manual intervention, which was inconsistent with our automation objectives. We may consider updating the process to include curvilinear grids in the future.

In small streams, surface roughness is primarily driven by the distribution of pebble sizes in the substrate. Because features at this spatial scale cannot be directly modeled, we accounted for surface roughness using the White-Colebrook model (Colebrook and White, 1937; Colebrook, 1939). We use D84 as a proxy for surface roughness. We experimented with different scalars applied to D84 as the surface roughness input to the roughness model, and optimized around this scalar (see section 2.5).

Initial conditions for the model are set such that the water level at all points is equal to the water level at the downstream boundary condition. We found that the steady state solution was not dependent on initial conditions.

To ensure our computational solutions reach steady state, we estimate the volume of water present in the reach from the DEM and water surface elevation digital elevation model (WSEDEM) and then run the simulation until the rate of discharge multiplied by the simulation time is equal to twice the total water volume of the reach. We find this always provides ample margin, ensuring simulations reach steady state.

The master definition file is a key input file used to run Delft flow and lists the names and locations of all input files (Table 1), surface roughness (D84), and constants describing the physical properties of freshwater (Deltares, 2013a). This file is generated by the pre-processing script after all other input files are generated, simulation time has been determined, and surface roughness inputs are determined.

2.3.3 Step 3: set up batch processing

Delft Flow is run in batch mode, bypassing any need for manual operation. A .csv file containing a list of reach visits, discharges, and surface roughness (D84), and file locations for DEM, WSEDEM, and thalweg files is user generated and read by the pre-processing R code. A batch file is also generated that is used to convert Delft Flow output into text files (step 5).

2.3.4 Step 4: run Delft Flow

Once all pre-processing is complete, Delft Flow is run for a batch of surveys; time required for each reach to be modeled ranges from a few minutes to several hours, and we use typical batch sizes of 20 to 50 reaches. Models are run using elastic cloud computing (EC2 service, Amazon Web Services, https://aws.amazon.com/) and all required survey data inputs are stored in Amazon storage buckets (S3) in .csv formats. As many EC2 instances as needed are generated, and there is unlimited potential to scale computing resources. We typically used the instance type “C4.4xlarge” as it provides sufficiently fast computing with sufficient memory to run up to 50 models in a single batch, at otherwise minimum costs ($0.796 per hour per instance, as of November 2017). Modeling thousands of reaches locally would not have been practical, and Amazon Web Services was an effective tool to provide cost effective computational power. Model outputs are saved for from 10 evenly dispersed time steps throughout the simulation and these can be used to ensure the flow reaches a steady state.

2.3.5. Step 5: converting Delft flow output to .txt format

Delft Flow output is not readable by R or other common data viewers, so we use the viewer selector tool (vs.exe of the Delf3D flow suite, Deltares 2013b) and the batch file generated in step 3 to produce output files in text format for each model. These output files contain the X-location, Y-Location, X-velocity component, Y-velocity component, bottom elevation, water surface elevation, and dry points of each hydraulic model.

2.3.6. Step 6: post processing: translating model outputs onto original DEM grid locations and generating quality assurance plots

The viewer selector output text files are read into R and the velocity and depth results from these files are then interpolated back onto the original 10 cm DEM grid. The viewer selector tool exports files (X-velocity, Y-velocity, and water surface elevation) with data points that are not all reported at the same grid locations. Depths are reported at cell centers, while X-velocity and Y-velocity components are reported at half grid increment offsets in the X and Y directions, respectively (Deltares, 2013a). Interpolation is first done to translate velocity results to the computational grid centers, then both velocity and depth and are interpolated to the original 10 cm DEM grid. To reduce file size, only points identified as wetted according to either the hydraulic model solution or to the original crew survey are included in the results file. Location, velocity and depth metrics are included as outputs for each grid point (Table 2)

Output	**Description**	**Units**
X, Y	Geographic Cartesian coordinates for Northing and Easting, respectively, in meters	m
X Velocity, Y Velocity	X and Y vector components of velocity	m/s
Velocity Magnitude	Magnitude of resultant velocity vector	m/s
Depth	Water depth	m
WSE	Elevation of water surface, above sea level	m
Bed Level	Elevation of bed, above sea level	m
Depth Error	Difference between surveyed depth and modeled depth	m

Table 2. Hydraulic modeling output written to each row of the .csv output file. Output file contains one row for each point on a uniform 10 cm rectilinear grid overlaying each reach

The post-processing script generates a series of contour plots displaying velocity, depth, and water surface elevation. Plots of spatially explicit estimates of error in modeled depth are also calculated as the difference between surveyed depth and modeled depth and provide an overview of model accuracy allowing quick visual assessment.

2.3.7 Step 7: perform quality assurance checks

Quality assurance checks to assess the accuracy of boundary conditions or flows that fail to wet the entire reach are performed after each batch run. Boundary condition issues are the most common problem observed, but are easily found via visual review of boundary condition plots. Results from reaches with erroneous boundary conditions are not finalized (Figure 5). In almost all cases, boundary condition issues can be fixed via manual specification of the boundary conditions. To date, we have been unable to model only a single reach from the more than 2200 field surveys.

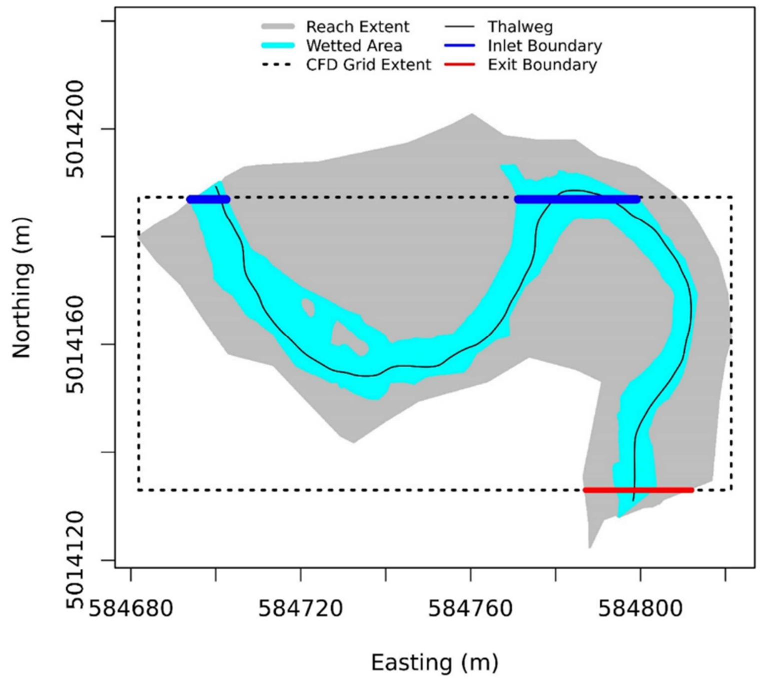

Figure 5. Boundary condition error resulting from failure of automated process. Manual specification of inlet boundary condition is required for this reach. Inlet boundary near middle of the reach is the erroneous boundary.

2.3.8 Step 8: upload results to database

Once model batches have been completed and quality assured, model results are uploaded to a centralized cloud storage system and sent to a central database repository (www.champmonitoring.org).

2.4 Model validation

In 2013 velocity and depth data were collected at points along 169 transects spread over 36 reaches. The validation reaches covered a broad variety of reach types and flow rates (mean = 0.63 m^3s^{-1}, sd = 1.59 m^3s^{-1}), and included reaches from the Asotin, Entiat, John Day, Lemhi, and

Tucannon watersheds (see Figure 2). At each reach, crews identified 3-6 validation transects. Each transect was divided into 15-20 equally spaced intervals where depth and depth-averaged velocity were measured. Measured depths and depth averaged measured velocities at each point along validation transects were compared to modeled depths and velocities. Also, the surveyed depths were compared to modeled depths across the entire wetted surface. Approximate depth averaged velocity measurements (at 60% of depth) were taken rather than full vertical profiles. This data collection decision was made to minimize field costs and in belief that it would support the type of two-dimensional modeling efforts previously used to develop HSI and NREI models.

2.5 Model optimization

In modeling of complex natural systems, it is impractical, both in terms of computational power and our ability to create DEMs at high enough precision, to include true features in a DEM that can be described as "surface roughness." Therefore we used the White-Colebrook model for surface roughness and assumed a scalar value of D84 provides a reasonable proxy for surface roughness. For calibration, we varied the scaling factor over a range of values from 1 to 8, and then compared resulting velocity and depth fields modeled at each scalar value to depths and velocities measured at a series of validation points at a subset of stream reaches. We selected our scalar on D84 to be used to input surface roughness as the value that minimized the overall error in validation.

Using a scalar multiplier on the metric D84 proved effective at calibrating the model. As the multiplier is increased, modeled depth tended to decrease, while modeled velocity tended to increase (Figure 6). At a D84 multiplier of approximately 3.0, velocity and depth errors were minimized. Because our intention was to model thousands of uniquely surveyed reach / visit combinations, we used this value for all reaches, rather than optimizing the scalar on a reach by reach basis.

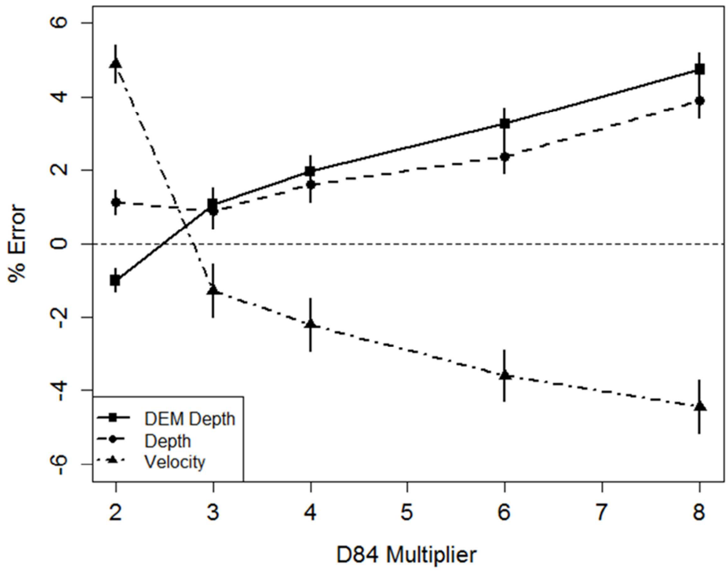

Figure 6. Estimated mean error at validation locations vs multiplier applied to scale D84 as surface roughness input to model. Error is defined as percent difference between modeled values for a) depth as measured in DEM survey, b) direct depth measurements at validation points, and c) direct velocity measurements at validation points. Vertical bars indicate 95% confidence bounds.

3.1 Results

To date, more than 2200 hydraulic models have been successfully run, representing multiple years of surveyed reaches. Based on a random subsample for which we tracked required computation times, the computational times averaged 64.0 minutes, with a standard deviation of 39.8 minutes. The minimum and maximum computational times from our subsample were 15.6

and 224.1 minutes, respectively. In general, it appeared that large reaches and reaches with low discharge rates required longer modeling times to reach a steady state. All computations were done using “C4.4xlarge” Amazon Web Service instances, which are powered by high frequency Intel Xeon E5-2666 v3 (Haswell) processors (Details available at https://aws.amazon.com/ec2/instance-types/).

To ensure our grid spacing was sufficiently fine, we compared simulation results at the grid spacing determined by our 500,000 cell limit to those run at coarser grid spacing across a variety of stream reaches. Varying grid spacing demonstrated that our grid spacing algorithm produces sufficiently fine grids. Doubling the grid spacing resulted in minor deviations in velocity fields (Figure 7) and corresponding depth fields. As grid spacing was further increased to 4X the default grid spacing, significant differences in velocity and depth fields occurred, indicating that that grid spacing would be too coarse.

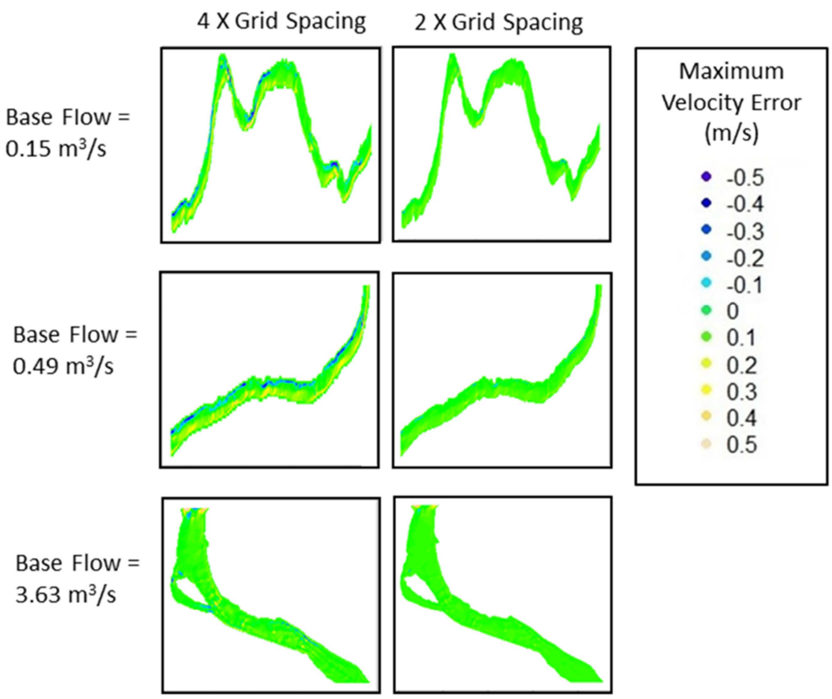

Figure 7. Velocity magnitude differences, relative to simulations at default grid spacing, for simulations performed at 4X and 2X default grid spacing, for low, medium, and high flow reaches.

3.2 Model validation

We used linear regression models to compare modeled depths to validation depths for each validation reach and survey depths (water surface elevation – DEM elevation) at all wetted channel survey points. Modeled depths were a significant predictor of measured depths for 73% of the validation transects (123 of 168 transects, $r^2 = 0.53$, $p < 0.05$). Modeled velocities were a significant predictor of measured velocities for 41% of the validation transects (69 of 168 transects, $r^2 = 0.39$, $p < 0.05$). Graphical comparisons of modeled results and validation data showed reasonably good agreement. The majority of reaches had only small amounts of error, relative to the total within reach variability, when comparing surveyed depths to modeled depths at each validation data transect within each reach (Figure 8d). Similarly, the distribution of velocity and depth values at validation points matched reasonably well between modeled and measured values (Figure 9). In almost all cases, modeled velocity and depth profiles were much smoother and showed lower levels of localized variability than the depths and velocities measured at validation points. This was expected since the survey process produces a DEM that lacks spatial variability at spatial scales as small as features such as rocks, cracks, and woody debris. Because the DEM on which the model is calculated is considerably less locally variable than the actual bathymetry, the modeled depths and velocities lack the localized variability captured by manual validation measurements.

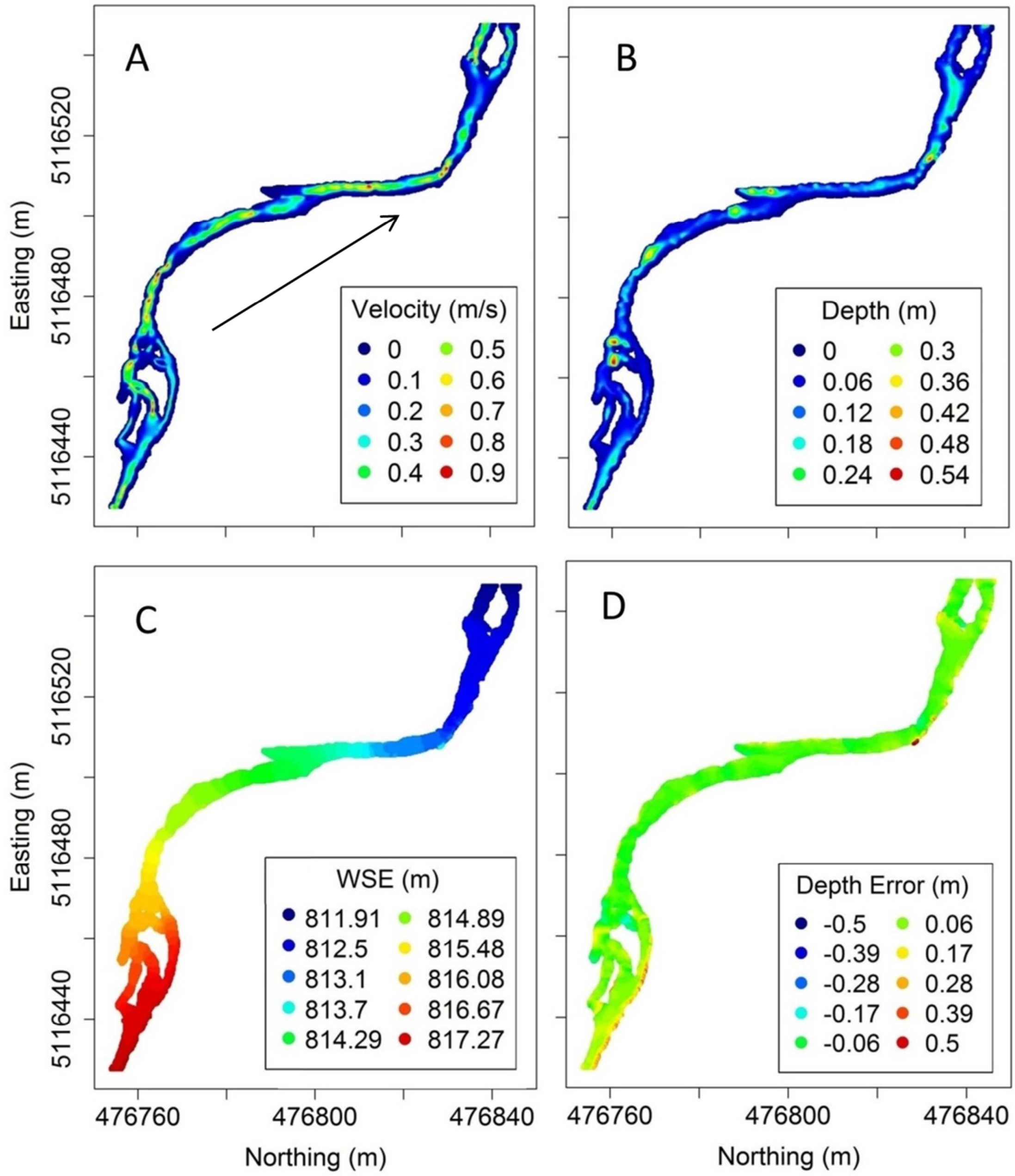

Figure 8. Velocity (A), depth (B), surface elevation (C), and depth error estimated as difference between surveyed depth and modeled depth (D), for reach ASW00001-SF-F5_P3BR. Arrow in (A) indicates flow direction.

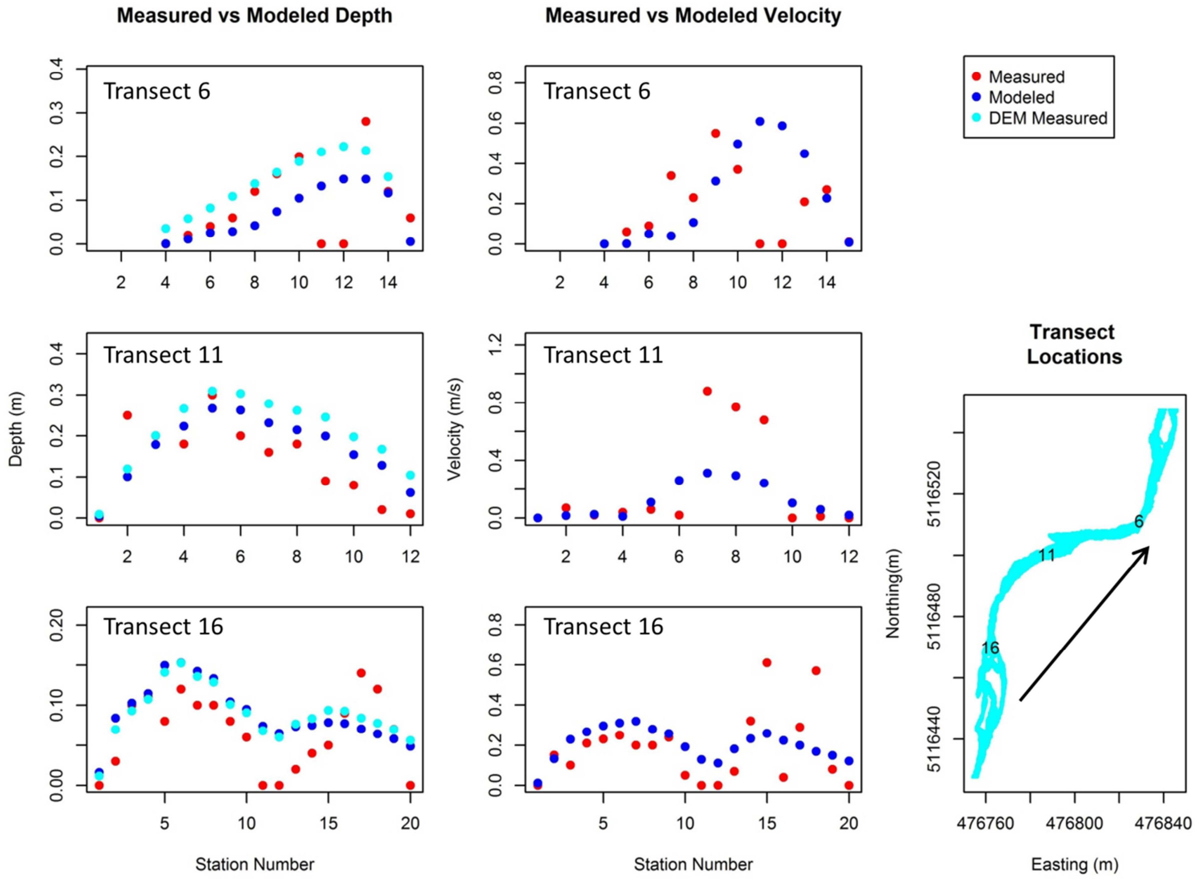

Figure 9. Example modeled depth and velocity compared to measured depth and velocity at validation points. DEM measured depth is depth derived from DEM survey. Measured depth and velocity are direct measurements at transect locations. Arrow indicates flow direction. Note that some number of transect points varies with stream width at transect.

Comparing modeled depths to crew-surveyed depths resulted in better agreement than to validation data depths. When we examined these at the same transect points of the validation data, we found modeled depths were a significant predictor of crew-surveyed depths for 100% of the validation models (168 transects, $r^2 = 0.973$, $p < 0.05$). This result was expected as the model was based on the crew-surveyed data.

Since habitat capacity models are often aggregated to a reach scale (e.g. average depth, NREI, or HSI for an entire reach), we reviewed model performance among reaches by comparing average depth and velocity values among measured and modeled results. Average reach velocity and depth were both strongly correlated between validation and modeled points ($r^2 = 0.93$ (Figure 10a) and 0.90 (Figure 10b), respectively). Correlations of surveyed to modeled depths and validation depths also produced high r^2 values of 0.85 (Figure 10c) and 0.87 (Figure 10d), respectively. This suggested that survey precision was generally acceptable and localized variation observed in validation data does not appear to measurably affect reach-scale averages.

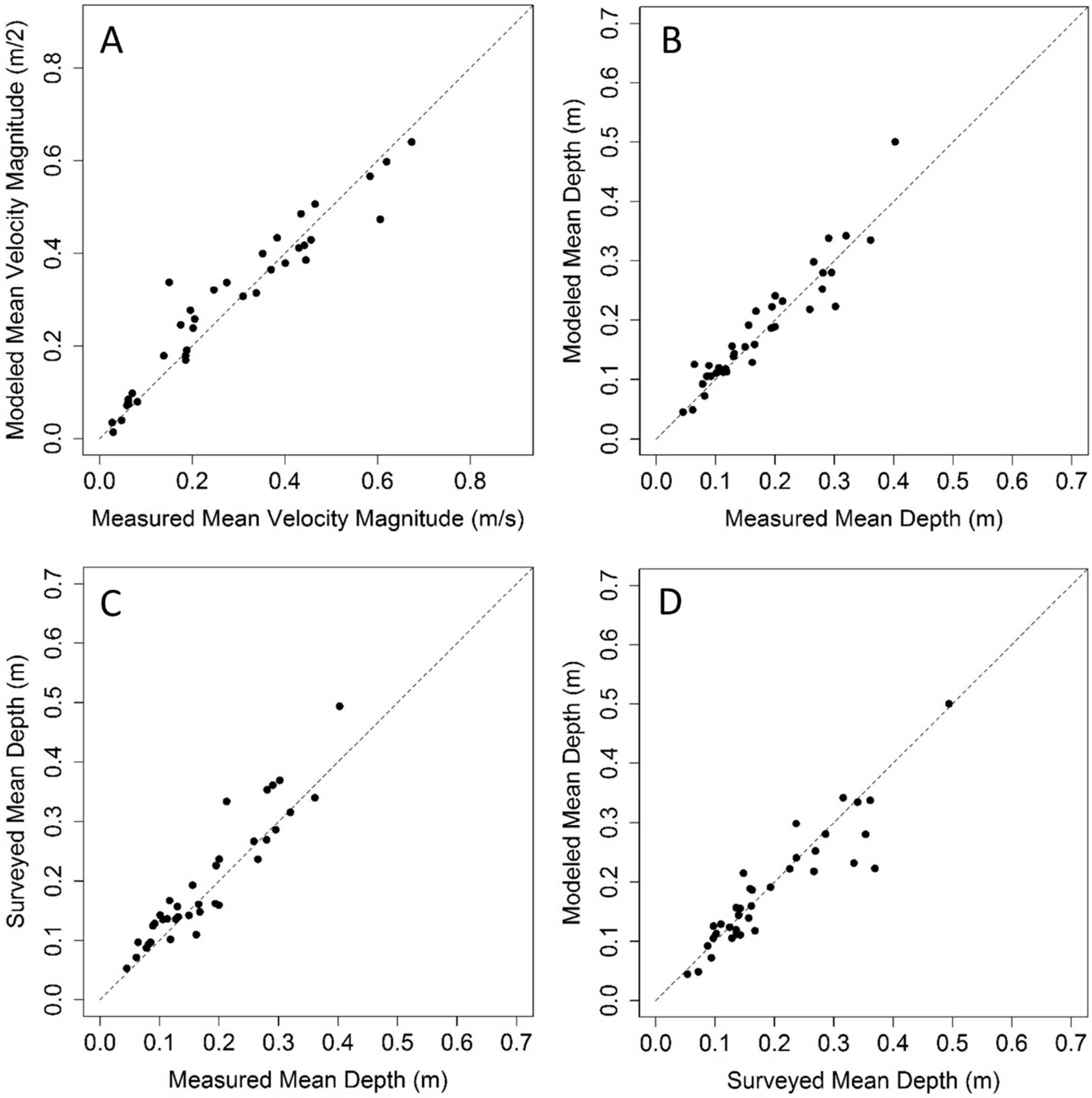

Figure 10. Reach level validation: measured versus modeled velocity (a), depth (b); modeled versus surveyed depth (c), and measured versus surveyed depth (d). Each point represents a reach average; all reaches where validation data were taken are included.

3.3 Model Limitations

Although modeled results were generally in agreement with validation data, we have found cases where the presence of non-bathymetric features affecting hydraulics caused localized, inaccurate model results. Such features included undercut banks and large, sometimes porous, woody structures. While undercut banks and porous woody structures are assessed as part of the sampling protocol used to generate our input data, these features were not included in the topographic surveys and therefore not included in the DEM. As a result, their impacts to the depth and velocity fields were not reflected in the hydraulic models.

For example, at a reach in the Entiat (WA) the survey crew noted a large tree that had fallen across part of the channel. The hydraulic model did not account for this, and we found large, localized depth field errors upstream of the fallen log (Figure 11).

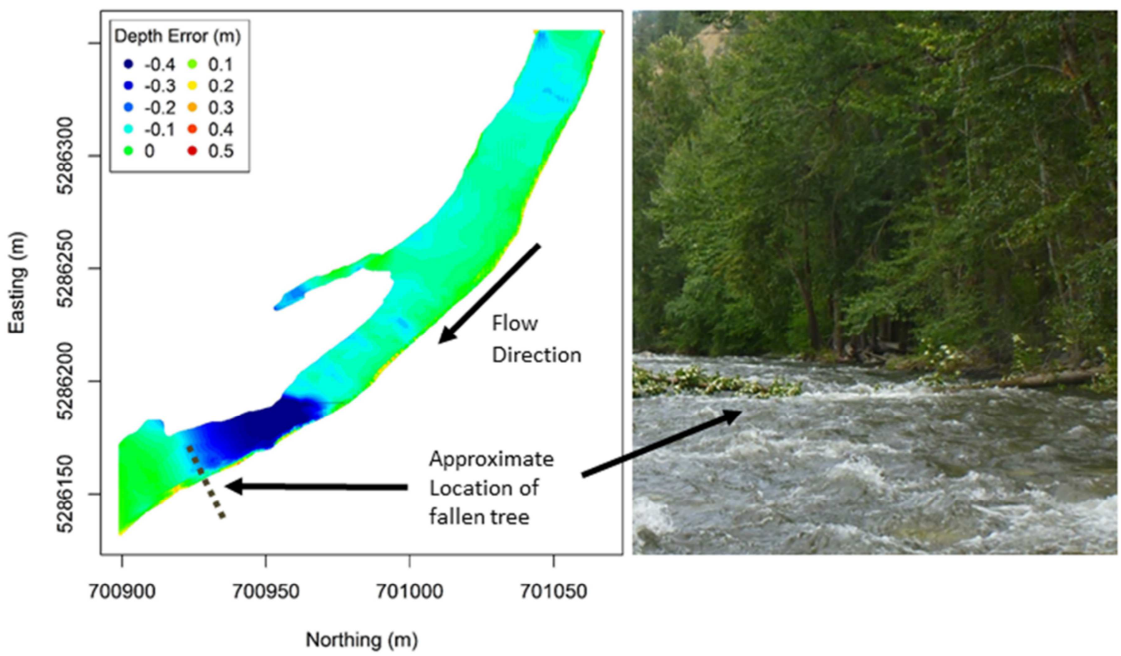

Figure 11. Depth error, with respect to surveyed depth, for reach ENT0001-1E3. Localized area where modeled depth is underestimated, likely due to a fallen log in river.

Logs, shrubs, and other woody debris is not reflected in DEM, thus increase in water surface elevation upstream from log is not reflected in the hydraulic model.

Undercuts were another feature not represented in topographic inputs and therefore not accounted for in hydraulic model results. Modeled DEMs of reaches with undercuts reflect stream banks that run vertically down from the edge of the overhanging bank, rather than an undercut bank. At a reach in the Asotin (WA), the crew observed a considerably undercut bank. The modeled reach has a smaller wetted cross sectional width than in reality. The modeled flow was more constrained than the actual flow, and the resulting modeled depth was greater than the actual depth near the undercut location (Figure 12).

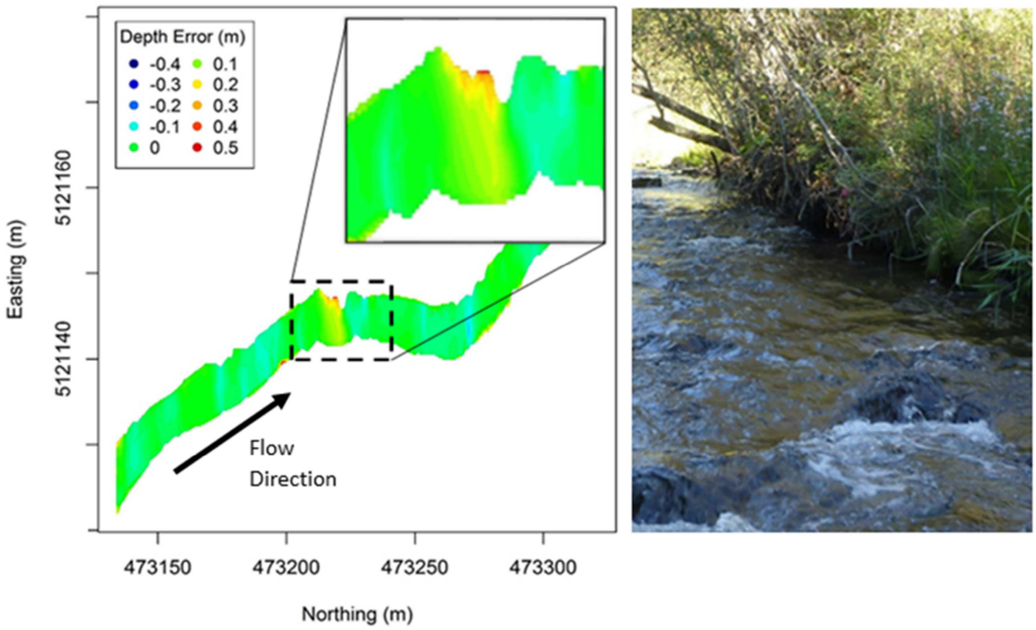

Figure 12. Depth error, with respect to surveyed depth, for reach ASW00001-NF-F4_P1BR. Undercut bank, on river left, is not reflected in DEM, thus hydraulic model

over predicts depth because modeled cross sectional area is less than actual cross sectional area, by amount of area in undercut.

In addition to the limitations discussed above, we recognize that there are small features (at scales of less than 30-50 cm) that are important stream habitat and very localized flow conditions that our modeling approach cannot predict, both because we utilize a 2D depth averaged model and because the feature size captured in the input DEMs is generally larger than 10 cm. Nevertheless, previous research has indicated that hydraulic modeling at the scale of the features captured at this scale in depth averaged mode, can provide useful information regarding habitat capacity at the reach scale (Hayes et al., 2007). By enabling habitat capacity estimates at this precision level, for high numbers of reaches, reach level habitat models (HSI, NREI) can be upscaled to inform salmonid population life cycle models (Wheaton et al, 2017).

4.1 Discussion

We have successfully generated accurate and precise hydraulic models for more than 2200 field surveys, covering more than 900 unique reaches, producing estimates of depth and velocity fields. These products have been instrumental in the development of high resolution models estimating energetic capacity and habitat suitability for salmonids (Wall et al. 2016; Wheaton et al. 2017; McHugh et al. 2017)

We have met our objectives of modeling large numbers of reaches with varied physical features and geometries with a practical, efficient method. Models may also be manually adjusted to meet explicit needs of individual reach conditions, such as flow adjustments for side channels, reduced boundary conditions, or to model non-measured flow conditions. Our simplistic approach in processing, parameter, and batch-mode utilization limited the amount of required manual intervention, generally at the expense of computational efficiency. For example, we used simple rectilinear computational grids rather than curvilinear or adaptive mesh grids and our grid spacing was often finer than needed for much of the modeled flow. However, given the abundance of computational power available, it was more effective to use simple rectilinear grids at the expense of computational efficiency, rather than add the complexity of automating and validating curvilinear grids for every reach. We also automated the grid spacing algorithm to enable automation over individual model level optimization and found our automated algorithm to be sufficient. Trimming a small amount of the surveyed reach out of the computational domain represents another tradeoff that enables modeling of high numbers of reaches. Slight reductions in the spatial extent modeled helps to enable automated generation of boundary conditions, as is required for process automation. The series of modeling choices we made during process development (Table 3) are common to most hydraulic modeling efforts. However, our recommendations are specific to the needs of our end users (primarily developers of HSI and NREI habitat models) and the need to model 1000s of individual reaches. Modelers facing different challenges may reach different processing decisions.

Decision	**Primary Considerations**	**Recommendations***
Modeling Software	Cost, usability, 2D vs 3D capabilities	Delft Flow
2D versus 3D	Spatial resolution of input data, uses for hydro model results, computational power available	Depth Averaged 2D
Curvilinear or Rectangular Grid	Automation requirements, sensitivity to boundary condition errors	Rectangular

Computational Grid Spacing	Feature size captured by survey, size of reach	Create grid as fine as possible within memory requirements
Batch processing (automated) vs manual processing	Number of models required	Batch processing
Cloud computing or local processing	Number of models required	Cloud computing

* Recommendations based on our end user requirements: HSI and NREI models for 1000's of reaches

Table 3. Modeling choices made and recommendations

Within individual reaches, we generally found modeled depths reflected surveyed depths better than validation depths. Since the hydraulic model is based on survey information, this suggests that topographic survey precision may be the limiting factor of hydraulic model accuracy. Nevertheless, we find that hydraulic model results generally account for much of the variation observed in validation data. At the reach scale, we found excellent agreement between reach scale average velocities and depths when comparing average modeled results at validation points to our validation data.

Using cloud computing was crucial in enabling us to meet our automation objectives. It simply would not be feasible or cost effective to run thousands of hydraulic models on an individual computer or a fixed collection of computers.

Our hydraulic modeling process provides both a streamlined modeling process and a core bathymetric dataset that can be used to quantify the effect of habitat restoration on salmonid population dynamics. Restoration scenarios can be mimicked by altering measured DEMs, modifying discharge rates to simulate restored flows, or changing surface roughness to model changes in surface features (Wall et al. 2016). This enables not only a quantitative comparison of multiple restoration options, but a methodology for optimizing restoration given a restoration strategy. This simplified hydraulic modeling process is an accessible and valuable tool for the exploration of future restoration scenarios.

Lessons learned during this process development include those applicable to field crews to improve topographic surveys. Future field data collection efforts should carefully define what feature sizes to include or exclude from the field survey and that information should be considered in modeling applications. Field crews could ensure upstream and downstream endpoints are at locations that will enable clean boundary conditions and avoid known problematic boundary locations (Figure 5). Inclusion of features obstructing hydraulic flows and improved undercut representation could also benefit hydraulic model products.

4.2 Future Work

Most of our hydraulic modeling efforts have focused on measured discharge during summer low-flow conditions. However, the hydraulic conditions at several times throughout a year can be important factors for salmonid habitat capacity. This modeling approach is well suited to modeling hydraulic conditions for discharges at these key times of year. This would allow estimation of energetic capacity and habitat suitability to inform salmonid habitat availability during multiple life stages. Porous structures, including large woody debris, beaver dams, undercuts, and similar features are important to salmonids and other fish species (Majerova et al.,

2015) and are often part of habitat restoration strategies (Bouwes et al., 2016; Bennett et al., 2016), but are not well represented by the DEMs used in our model development. Developing strategies for simulating such structures will provide additional flexibility in restoration scenario development and could pinpoint additional features to include in field surveys.

Using rectangular computational grids instead of curvilinear computational grids was one of our major tradeoffs, and we knowingly accept an increase in boundary condition error at the upstream and downstream ends of our modeled reaches. Future work may reconsider this tradeoff through development of automated curvilinear grid generation methods that rarely require manual intervention.

Using cloud computing resources was critical to model implementation, and further cost reductions and speed improvements can likely be found by moving to Linux based computing and utilizing Amazon "spot" instances, where users bid on available instances, possibly decreasing computational costs by an order of magnitude.

Ultimately, the hydraulic modeling process (from field data collection to finished hydraulic models) is a compromise between localized accuracy and precision and the need to estimate habitat throughout entire watersheds. All projects considering large-scale production of hydraulic models should consider tradeoffs between local spatial precision, watershed coverage, and resource constraints. Questions around modeling cost, development, and precision are likely to continue with technological advances in LiDAR and remote sensing that can inform and offer hydraulic modeling options: "Should more resources go toward obtaining finer scale field data and developing higher precision, three dimensional hydraulic models and habitat models, likely at the expense of overall sample size?" Similarly, "should (possibly) lower resolution field data covering a more complete subsample of watersheds of interest be used to develop broader, but perhaps less locally precise hydraulic models?" Ultimately the answers to these questions are likely project-specific, balancing project objectives and needs with resources and resolution.

Acknowledgements

This work was accomplished as part of Bonneville Power Administration Fish and Wildlife projects (#2003-017-00 and #2011-006-00) and was supported by the National Oceanic and Atmospheric Administration, National Marine Fisheries Service and Utah State University. We would also like to acknowledge the CHaMP field crews that collected field and validation data. Finally, we acknowledge the reviewers for contributing their time and efforts.

References

Bangen, S., 2013. Comparison of Topographic Surveying Techniques in Streams. All Graduate Theses and Dissertations. 1516. https://digitalcommons.usu.edu/etd/1516

Bangen S., Wheaton J.M., Bouwes N., Jordan C., Volk C., Ward M.B., 2014. Crew variability in topographic surveys for monitoring wadeable streams: a case study from the Columbia River Basin. Earth Surface Processes and Landforms, 2014.

Benjankar, R., Tonina, D., McKean, J.A., Sohrabi, M.M., Chen, Q., Vidergar, D., 2018. Dam operations may improve aquatic habitat and offset negative effects of climate change. Journal of Environmental Management, Volume 213, 1 May 2018, Pages 126-134, https://doi.org/10.1016/j.jenvman.2018.02.066

Bennett S., Pess G., Bouwes N., Roni P., Bilby R.E., Gallagher S., Ruzycki J., Buehrens T., Krueger K., Ehinger W., Anderson J., Jordan C., Bowersox B., Greene C., 2016. Progress and Challenges of Testing the Effectiveness of Stream Restoration in the Pacific Northwest Using Intensively Monitored Watersheds, Fisheries, 41:2, 92-103, DOI: 10.1080/03632415.2015.1127805

Booker, D.J., Dunbar M.J.; Ibbotson A., 2004. Prediction juvenile salmonid drift-feeding habitat quality using a three dimensional hydraulic-bioenergetic model. Ecol. Model. 177: pp 157-177

Bouwes, N., Moberg, J., Weber, N., Bouwes B., Bennett, S., Beasley C., Jordan, C., Nelle, P., Polino M., Rentmeester, S., Semmens B., Volk, C., Ward M.B., White, J., 2011. Scientific protocol for salmonid habitat surveys within the Columbia Habitat Monitoring Program. Terraqua, Inc., Wauconda, WA.

Bouwes N., Bennett S., Wheaton J., 2016. Adapting Adaptive Management for Testing the Effectiveness of Stream Restoration: An Intensively Monitored Watershed Example, Fisheries, 41:2, pp 84-91, DOI: 10.1080/03632415.2015.1127806

Brasington, J., Rumsby, B., McVey, R., 2000. Monitoring and modelling morphological change in a braided gravel-bed river using high resolution GPS-based survey. Earth Surface Processes and Landforms 25 (9), 973–990

CHaMP, 2015. The Columbia Habitat Monitoring Program: 2013 Third Year Lessons Learned Project Synthesis Report 2011-006-00. Prepared by CHaMP for the Bonneville Power Administration. Published by Bonneville Power Administration. 67 pages.

Colebrook, C.F., 1939. Turbulent flow in pipes, with particular reference to the transition region between smooth and rough pipe laws. Journal of the Institution of Civil Engineers (London).

Colebrook, C. F., White, C. M., 1937. Experiments with Fluid Friction in Roughened Pipes. Proceedings of the Royal Society of London. Series A. Mathematical and Physical Sciences 161 (906): pp 367–381.

Deltares, 2013a. Delft3D-FLOW: Simulation of multi-dimensional hydrodynamic flows and transport phenomena, including sediments. User Manual. Version: 3.15.26466.

Deltares, 2013b. Viewer Selector: Inspection, selection and retrieval of data from a NEFIS File, User Manual, Version: 1.23.23866

Fuller, I., Large, A., Charlton, M., Heritage, G., Milan, D., 2003. Reach-scale sediment transfers: an evaluation of two morphological budgeting approaches. Earth Surface Processes and Landforms 28 (8), 889–903.

Gupta, H. V., Sorooshian, S., Yapo, P. O., 1999. Status of automatic calibration for hydrologic models: Comparison with multilevel expert calibration. Journal of Hydrologic Engineering, 4(2), pp 135-143. DOI: 10.1061/(ASCE)1084-0699(1999)4:2(135)

Hayes, J.W., Hugues, N.F., Kelly, L.H., 2007. Process-based modelling of invertebrate drift transport, net energy intake and reach carrying capacity for drift-feeding salmonids, Ecological Modelling 207.

Kelly, L.H., Hay, J., Hughes, N.F., Goodwin, E., and Hayes, J.W., 2012. Flow related models for simulating river hydraulics, invertebrate drift transport, and foraging energetics of drift-feeding salmonids: user guide (version 1.1). Cawthron Report 922.

Lacey, R.W.J., Millar, R. G., 2004. Reach scale hydraulic assessment of instream salmonid habitat restoration. Journal of the American Water Resources Association, 40: 1631–1644. doi:10.1111/j.1752-1688.2004.tb01611.x

Leclerc, M., Boudreault, A., Bechara, J.A., and Corfa, G., 1995. Two-dimensional hydrodynamic modeling: A neglected tool in the instream flow incremental methodology, Trans. Am. Fish. Soc., 124, 645–662, doi:10.1577/1548-8659(1995)124<0645:TDHMAN>2.3.CO;2.

Majerova, M., Neilson, B.T., Schmadel, N.M., Wheaton, J.M., and Snow, C.J., 2015, Impacts of beaver dams on hydrologic and temperature regimes in a mountain stream, Hydrol. Earth Syst. Sci., 19, 3541–3556, doi:10.5194/hess-19-3541-2015

Maret, T.R., Hortness, J.E., Ott, D.S., 2006. Instream flow characterization of upper Salmon River basin streams, central Idaho, 2005. Scientific Investigations Report 2006-5230. U. S. Geological Survey: 110.

McHugh P., Saunders C., Bouwes N., Wall E., Bangen S., Wheaton J., Nahorniak M., Ruzycki J., Tattam I. and Jordan C., 2017. Linking models across scales to assess the viability and restoration potential of a threatened population of steelhead (*Oncorhynchus mykiss*) in the Middle Fork John Day River, Oregon, USA. Ecological Modelling, 355: pp 24-38. DOI: 10.1016/j.ecolmodel.2017.03.022.

Moussalli, E., Hilborn, R., 1986. Optimal Stock Size and Harvest Rate in Multistage Life-

History Models. Canadian Journal of Fisheries and Aquatic Sciences. 43(1): 135-141. DOI: Doi 10.1139/F86-014.

Olivera, F., and Maidment, D.R., 2000. GIS tools for HMS modeling support. Hydrologic and hydraulic modeling support with geographic information systems. Environmental Systems Research Institute Press, USA. 216 pp.

Pasternack, G.B., Gilbert, A.T., Wheaton, J.M., Buckland, E.M., 2006. Error Propagation for Velocity and Shear Stress Prediction: Using 2D Models for Environmental Management. Journal of Hydrology Volume 328, Issues 1–2, pp 227–241.

R Core Team, 2014. R: A language and environment for statistical computing. R Foundation for Statistical Computing, Vienna, Austria. URL http://www.R-project.org/.

Rubin, S.P., Bjornn, T.C., Dennis, B., 1991. Habitat suit-ability curves for juvenile Chinook salmon and steelhead developed using a habitat-oriented sampling approach: Rivers. 2(1):12-29.

Schwartz J.S., Keil J.N., Dworak F.E., Woockman R.R., 2015. Restoring riffle-pool structure in an incised, straightened urban stream channel using an ecohydraulic modeling approach. Ecological Engineering, Volume 78, pp 112-126.

Shen, Y. and Diplas, P., 2008. Application of Two- and Three-dimensional Computational Fluid Dynamics Models to Complex Ecological Stream Flows. Journal of Hydrology, 348(1-2): pp 195-214.

Stevens Jr, D.L., Olsen, A.R., 2004. Spatially balanced sampling of natural resources. J Am Stat Assoc, 99:465, 262-278, DOI: 0.1198/016214504000000250.

Tranmer, A.W., Marti C.L., Tonina, D., Benjankar, R., Weigel, D., Vilhena, L., McGrath, C., Goodwin, P., Tiedemann, M., Mckean J., Imberger, J. A hierarchical modelling framework for assessing physical and biochemical characteristics of a regulated river. Ecological Modelling Volume 368, 24 January 2018, Pages 78-93. https://doi.org/10.1016/j.ecolmodel.2017.11.010

Tullos, D., Walter, C., Dunham, J., 2016. Does resolution of flow field observation influence apparent habitat use and energy expenditure in juvenile coho salmon? Water Resources Research, DOI 10.1002/2015WR018501.

Wall, C.E., Bouwes, N., Wheaton, J.M., Bennett, S.N., Saunders, W.C., McHugh, P., Jordan, C.E., 2016. Design and monitoring of woody structures and their benefits to juvenile steelhead trout (Oncorhynchus mykiss) using a net rate of energy intake model. Canadian Journal of Fisheriesand Aquatic Sciences. DOI:10.1139/cjfas-2016-0131.

Wheaton, J.M., Brasington, J., Darby, S.E., Merz, J., Pasternack, G.B., Sear, D., Vericat, D., 2010. Linking geomorphic changes to salmonid habitat at a scale relevant to fish. River Research and Applications 26: pp 469–486.

Wheaton, J.M., McHugh, P., Bouwes, N., Saunders, W., Bangen, S., Bailey, P., Nahorniak, M., Wall, C., Jordan, C., 2017. Upscaling site-scale ecohydraulic models to inform salmonid population-level life cycle modelling and restoration actions – Lessons from the Columbia River basin. Earth Surface Processes and Landforms. Doi: 10.1002/esp.4137.

Yagecic, J., Suk, N., 2014. Automation of a Hydrodynamic Model of the Delaware Estuary for Rapid Water Quality Simulations of Pollutant Releases. Journal of the American Water Resources Association (JAWRA) 50(5): 1359-1364. DOI: 10.1111/jawr.12185

Highlights: How do we efficiently generate high-resolution hydraulic models at large numbers of riverine reaches?

- We present an automated process to generate hydraulic models for small stream reaches
- Automation of the hydraulic modeling is the novel advancement presented here.
- Tradeoffs made to enable high volume model generation are discussed
- Validation of model results shows that results are generally accurate